SIGNAL ATTENUATION CHARACTERISTICS AT THE PHYSICAL LAYER OF IoMT SYSTEMS, COMPARISON OF DIFFERENT SCENARIOS

Goran Popović[1], Almir Ahmetspahić[1]
[1]International University of Travnik, Faculty of Poliytechnic Sciences, Department of Electrical Engineering, Aleja konzula – Meljanac bb, 72270 Travnik, Bosna i Hercegovina,
e-mail: goran.popovic@iu-travnik.com, almir.ahmetspahic@iu-travnik.com

Izlaganje sa znanstvenog skupa
https://www.doi.org/10.58952/zr20261501310
UDK / UDC 621.396:004.738.5:61

Abstract
This paper presents the characteristics of signal attenuation at the physical layer of IoMT systems. The first two layers of the IoMT system (the physical PHY layer and the MAC data layer) are regulated by the IEEE 802.15.6 standard. In accordance with this standard, radio signal attenuation caused by the human body should be considered as an additional factor, alongside frequency and the distance between the transmitting (Tx) and receiving (Rx) antennas. The paper describes several different scenarios, as well as simulation results under realistic conditions for these scenarios. The scenarios differ in terms of sensor placement, the frequency bands they use, and the location of sensor installation relative to the patient's body. Based on the simulation results, the authors propose optimal solutions in terms of energy consumption optimization.
Keywords: *IoMT, Physical Leyer, Signal Attenuation, WBAN*
JEL: L630

INTRODUCTION

Inter-sensor communication in WBAN networks is influenced by a large number of factors that may degrade system performance and the stability of wireless channels. From the perspective of signal propagation, the human body consists of multiple natural absorption layers with different characteristics that affect the efficiency and radiation patterns of sensor nodes in different ways. Biological tissue is not a homogeneous dielectric medium, but rather a conductive and dispersive medium characterized by high relative permittivity and significant conductivity. Consequently, WBAN communication channels exhibit additional attenuation mechanisms, including electromagnetic energy absorption within biological tissue, creeping-wave propagation around the body surface, shadowing effects, and variations in propagation conditions caused by user movements. Implantable medical devices represent a particularly challenging scenario, since the transmitted signal must propagate through multiple tissue layers before reaching the external receiver. Under such conditions, significant path loss increase, signal-to-noise ratio degradation, and higher probability of data reception errors occur.

In order to standardize communication in WBAN systems, the IEEE 802.15.6 standard was developed, defining the physical and MAC layers for communication among medical and non-medical sensors operating in close proximity to the human body. The standard specifies multiple propagation scenarios, including communication between implantable sensors, between implantable and body-surface devices, between sensors located on the body surface, and communication between the body and external devices under LOS and NLOS conditions. Each of these scenarios exhibits different propagation characteristics and therefore requires a dedicated signal attenuation model.

In this paper, an advanced MATLAB-based simulation model of a WBAN/IoMT system was developed according to IEEE 802.15.6 propagation scenarios. The model incorporates frequency-dependent attenuation, the influence of dielectric properties of biological tissues, creeping-wave propagation, obstruction effects, signal-to-noise ratio analysis, BER estimation, energy efficiency evaluation, and SAR analysis. The simulation considers both implantable and body-surface sensors distributed across a human body model, while a smartphone is utilized as the external gateway device. Special attention is devoted to the comparison of different wireless technologies, including WiFi, Bluetooth, ZigBee, and MICS, with the objective of determining their suitability for various medical application scenarios.

The simulation results provide a detailed analysis of the influence of sensor placement, operating frequency, propagation scenario type, and communication technology on the overall performance of WBAN systems. Based on the obtained results, it is possible to define optimal solutions for energy-efficient and reliable transmission of medical data in IoMT environments.

1.COMMUNICATION MODELS

In WBAN networks, sensors may be positioned at different locations relative to the patient's body, which significantly affects their communication performance.

An implantable node is placed beneath the skin, either within deep biological tissues or directly under the skin surface. These nodes typically operate within the MICS (Medical Implant Communication Service) frequency band of 402–405 MHz. Electromagnetic energy absorption in such media increases with frequency due to higher dielectric losses and conductive dissipation. At higher frequencies, such as 2.4 GHz, the electromagnetic wave experiences significantly stronger attenuation, resulting in increased path loss, reduced communication range, and higher local tissue heating. In the frequency range around 400 MHz, the wave achieves better penetration, lower absorption per unit depth, and more stable propagation through layers of fat, muscle, and blood tissue. This enables a reliable communication link between the implant and the external receiver while requiring extremely low transmission power.

Strict output power limitations are imposed on these sensors in order to minimize interference and energy absorption within biological tissues. According to most standards, the maximum allowed transmission power is approximately 25 μW [3]. Such power limitations also extend battery lifetime, thereby reducing the frequency of replacement procedures, which are associated with surgical intervention. Furthermore, the MICS band is internationally reserved exclusively for medical implant communications, meaning that commercial systems such as WiFi or Bluetooth devices do not operate within this spectrum and therefore do not introduce interference. Implantable devices must not lose communication due to external disturbances, since they transmit vital physiological data such as cardiac rhythm, blood pressure, or neurostimulation parameters. An additional engineering compromise is related to antenna dimensions. Although the wavelength at 400 MHz is relatively large, the effective wavelength within biological tissue is significantly reduced due to high permittivity, enabling the design of miniaturized implantable antennas with acceptable physical dimensions.

Body-surface nodes are positioned directly on the human body or at a distance not exceeding 2 cm from its surface. These sensors predominantly utilize the 2.4 GHz ISM band through Bluetooth Low Energy (BLE) technology, which provides low power consumption, a standardized communication protocol, and direct integration with smartphones. In European environments, the 868 MHz band is also commonly used, offering improved propagation characteristics around the body due to lower frequency and reduced attenuation. Propagation over the body surface differs from free-space propagation because the electromagnetic wave may travel along the curved body surface through the creeping-wave phenomenon, thereby affecting field distribution and overall path loss. Sensor placement, antenna orientation, and the presence of clothing significantly influence link quality.

An external node is positioned in the vicinity of the human body, typically ranging from several centimeters up to a maximum distance of 5 m. In clinical systems, the external node may represent a specialized medical monitoring device, whereas in residential and commercial applications it is most commonly implemented as a smartphone or wearable device. Regardless of its physical form, its role is essential for the stability, reliability, and security of the entire WBAN architecture, since it acts as a bridge between biomedical sensors and the broader communication network. Such devices usually incorporate multiple RF interfaces in order to simultaneously support communication with different sensor categories, including both implantable and body-surface sensors.

Depending on the positions of the communicating sensors, WBAN network implementation includes seven possible communication scenarios (Figure 1):

- Scenario I: implant-to-implant, 402–405 MHz
- Scenario II: implant-to-body surface, 402–405 MHz
- Scenario III: implant-to-external sensor, 402–405 MHz
- Scenario IV: body surface-to-body surface LOS, 13.5, 50, 400, 600, 900 MHz, 2.4, 3.1–10.6 GHz
- Scenario V: body surface-to-body surface NLOS, 13.5, 50, 400, 600, 900 MHz, 2.4, 3.1–10.6 GHz
- Scenario VI: body surface-to-external sensor LOS, 900 MHz, 2.4, 3.1–10.6 GHz
- Scenario VII: body surface-to-external sensor NLOS, 900 MHz, 2.4, 3.1–10.6 GHz

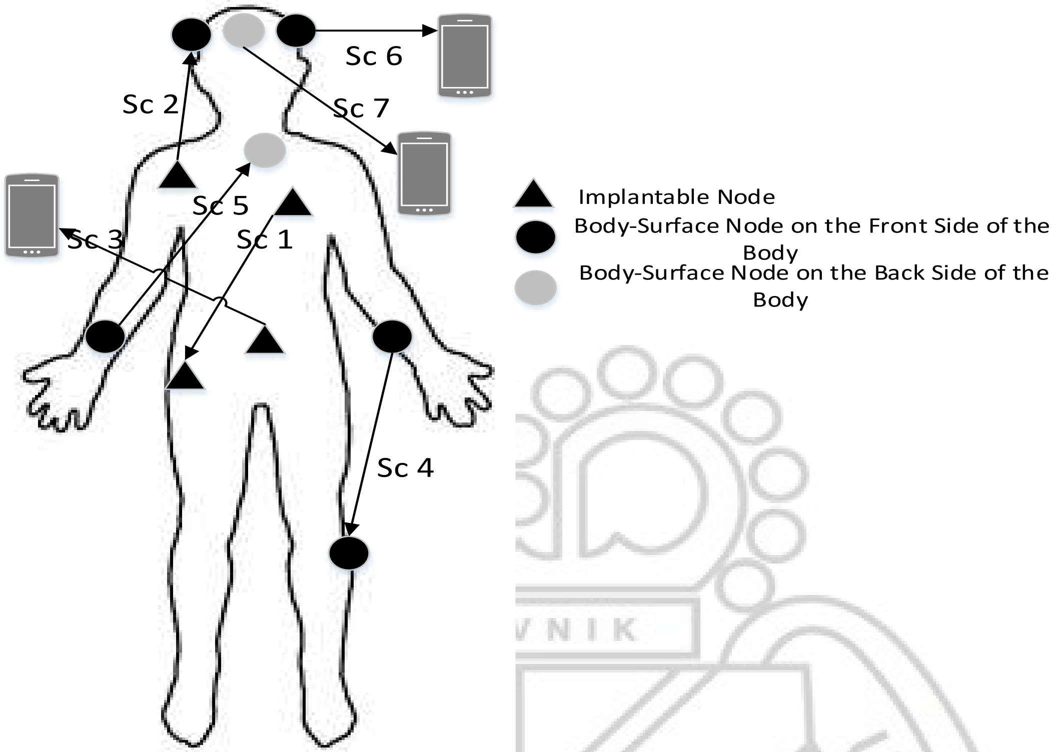

Figure 1. Sensor Node Placement Within the Human Body and Communication Scenarios

Path loss models strongly depend on electromagnetic phenomena as well as on the dielectric properties of biological tissues within the human body. In a simplified representation, the human body consists of three primary tissue types [1] (skin, adipose tissue, and muscle tissue), resulting in variable physiological and dielectric characteristics along the radio signal propagation path between the transmitter and the receiver in a WBAN network. The starting point for calculating the received signal power is the Friis transmission equation, which in its basic form can be expressed as:

$$P_r = P_t G_t G_r \left(\frac{\lambda}{4\pi d}\right)^2 \tag{1}$$

Where P_r denotes the received power [W], P_t is the transmitted power at the transmitting antenna [W], G_t represents the gain of the transmitting antenna, G_r is the gain of the receiving antenna, λ denotes the signal wavelength [m], and d is the distance between the transmitting and receiving antennas [m]. The term $4\pi d$ indicates that the electromagnetic wave radiated by the transmitting antenna propagates spherically in free space, meaning that the received power decreases proportionally to $1/d^2$. A shorter wavelength, i.e., a higher operating frequency, results in greater attenuation at the receiving point. This expression describes the relationship between transmitted and received power under free-space propagation conditions and is valid exclusively in the antenna far-field region, where the antennas are sufficiently separated, assuming direct line-of-sight (LOS) propagation, absence of reflections, diffraction, and absorption effects, as well as ideally matched impedances. In practice, the Friis equation is more commonly expressed in the following form:

$$P_r(dBm) = P_t(dBm) + G_t(dB) + G_r(dB) - L_{FS}(dB) \tag{2}$$

$L_{FS}(dB)$ represents the free-space path loss and is expressed as:

$$L_{FS}(dB) = 20log_{10}(d) + 20log_{10}(f) + 32.44 \quad (3)$$

where d is expressed in kilometers and f in MHz.

In WBAN networks, communication distances are typically in the meter range (0.1–2 m), while the 2.4 GHz ISM frequency band is frequently utilized for data transmission. Taking these values into account, the free-space path loss expression can be modified as follows:

$$L_{FS}(dB) = 20log_{10}(d) + 20log_{10}(f) + 92.44 \quad (4)$$

This expression represents a special case of the empirical log-distance path loss model:

$$L_{FS}(dB) = L_{FS}(d_0) + 10nlog_{10}\left(\frac{d}{d_0}\right) \quad (5)$$

where $L_{FS}(d_0)$ denotes the path loss at the reference distance d_0, while n is the path loss exponent. If expression (4) is evaluated at the reference distance d_0 and the obtained result is substituted into (5), the actual path loss value in the WBAN environment can be determined. The Friis equation is valid for larger distances when $n = 2$, whereas in WBAN environments the value of n is typically in the range of 3–4. The WBAN environment, consisting of the human body and surrounding objects that strongly absorb the signal, together with continuous body motion relative to the environment and time-varying changes in the relative positions of different body parts, causes variations in signal attenuation. Therefore, in a realistic environment, expression (5) can be represented as:

$$L_{FS}(dB) = L_{FS}(d) + S \quad (6)$$

where S represents a random variable introduced to account for shadowing-related effects and is typically modeled as a stochastic variable. Signal attenuation depends not only on the distance between the transmitter and the receiver, but also on the variability of dielectric properties of biological tissues along the propagation path. The dielectric properties of the human body relevant to WBAN communication channels include tissue permittivity (ε_r) and tissue conductivity (σ).

Scenario I: Implant-to-Implant Communication

The communication link between two implantable sensors in a WBAN network is typically established within the 402–405 MHz Medical Implant Communication Service (MICS) band and is characterized by specific propagation and system constraints that significantly affect the design of the physical layer and communication protocols [4]. This frequency range is utilized because radio waves within this band provide relatively good penetration through biological tissue compared to higher frequencies. Nevertheless, substantial losses still occur due to the dielectric properties of biological tissues, which can be modeled using complex permittivity, $\varepsilon = \varepsilon' - j\varepsilon''$. Typical values of relative permittivity for muscle tissue within this frequency range are $\varepsilon_r \approx 50$–60, while tissue conductivity is approximately $\sigma \approx 0.7$–1 S/m. Propagation between two implantable devices (the in-body channel) can be approximated using an exponential attenuation model:

$$L(dB) = L_{FS(d_0)} + 10nlog_{10}\left(\frac{d}{d_0}\right) + \alpha d \quad (7)$$

where $L_{FS}(d_0)$represents the reference path loss at distance d_0, $n$is the path loss exponent (typically ranging from 4 to 7 in biological tissue), and αdenotes an additional absorption coefficient dependent on frequency and tissue type [5].

Total propagation losses may reach 60–100 dB even at distances of only a few centimeters, imposing strict requirements on receiver sensitivity and overall link budget design. The communication channel between implantable sensors is generally quasi-static, with slow temporal variations caused by body movements, thereby enabling the application of adaptive techniques such as transmission power control and adaptive data rate adjustment. Typical data rates within the MICS band range from several kbps to several hundred kbps, which is sufficient for the majority of medical telemetry applications.

Scenario II: Implant-to-Body-Surface Communication

The communication link between an implantable sensor and a body-surface sensor within a WBAN system involves the transition of an electromagnetic wave from a highly dissipative biological medium into the external environment. This communication link is also most commonly realized within the 402–405 MHz frequency band, since this range provides a favorable compromise between tissue penetration capability, antenna dimensions, and regulatory constraints. In this scenario, the propagation channel may be considered as a cascade of two subsystems: (i) in-body propagation through the layered structure of biological tissues (muscle, fat, bone, and skin), and (ii) transmission across the tissue–air interface, followed by on-body or off-body signal propagation. In the first segment, losses caused by the dielectric properties of biological tissues dominate, leading to significant absorption and energy dissipation. Signal attenuation increases with implantation depth and may be modeled using a combination of logarithmic and linear components, where the total losses frequently reach 40–80 dB for typical propagation distances of several centimeters to the body surface. At the tissue–air boundary, additional reflections occur due to the large impedance mismatch, resulting in partial energy loss and modifications of the effective radiation pattern of the implantable antenna. This interface plays a crucial role in determining the overall link budget, since only a portion of the electromagnetic energy can be efficiently radiated outside the body. After emerging from the body, the signal propagates along the body surface and through free space toward the on-body sensor, while multipath effects, including reflections from the torso, limbs, and surrounding environment, may contribute to signal fluctuations.

Compared to alternative technologies such as Bluetooth Low Energy or ZigBee operating at 2.4 GHz, the MICS/MedRadio communication link between implantable and body-surface sensors provides significantly higher reliability due to lower tissue absorption. However, these technologies are often employed as secondary communication links between body-surface sensors and external devices (e.g., smartphones), thereby enabling a hierarchical WBAN system architecture. In this scenario, path loss can be expressed using the following semi-empirical model:

$$L(dB) = L_{FS}(d_0) + 10n\log_{10}\left(\frac{d}{d_0}\right) + \alpha d + L_{\text{int}} + L_{\text{ext}} \tag{8}$$

where: L_{int} represents the losses occurring at the tissue–air interface, while L_{ext} denotes the additional propagation losses along the body surface and in free space. According to [6], the following typical values are proposed: $L_{\text{int}} \approx$ 6–8 dB, $L_{\text{ext}} \approx 18.6$ dB

Scenario III: Implant-to-External Sensor Communication

The communication link between an implantable sensor and an external receiver located at a distance ranging from several centimeters up to a maximum of 5 m from the body, operating within the 402–405 MHz frequency band, represents a hybrid propagation scenario that includes electromagnetic wave propagation through biological tissue, transmission across the tissue–air interface, and subsequent propagation through free space in the vicinity of the human body.

After propagating through the body and crossing the boundary between the biological medium and air, the electromagnetic wave propagates through free space toward the external sensor, where the Friis propagation model may be applied. At a frequency of 403 MHz, the wavelength is approximately 0.74 m, resulting in free-space losses of approximately 32–34 dB at a distance of 5 m. This propagation segment becomes the dominant contributor to the overall attenuation for larger distances between the body and the receiver. Additionally, the presence of the human body introduces diffraction and absorption effects, commonly referred to as body shadowing and creeping-wave propagation, which produce additional losses in the range of 5–15 dB depending on the receiver position relative to the body.

The total path loss between the implantable transmitter and the external receiver can be modeled as:

$$L = L_{FS} + L_{\text{in}} + L_{\text{int}} + L_{\text{body}} \quad (9)$$

where: L_{in} denotes tissue losses associated with in-body propagation, L_{int} represents losses at the tissue–air interface, and L_{body} corresponds to additional body-related propagation effects. Reference [7] states that: $L_{\text{in}} = 8.686 \cdot \alpha d, L_{\text{int}} \approx 6\text{–}10\ \text{dB}, L_{\text{body}} \approx 5\text{–}15\ \text{dB}$

Scenario IV: Body Surface-to-Body Surface LOS Communication

The communication link between two sensors positioned on the body surface under line-of-sight (LOS) conditions represents a scenario in which the electromagnetic wave predominantly propagates along the body surface and through the surrounding near-body free space. Unlike in-body or implant-to-external communication scenarios, there is no propagation through deep biological tissues; however, the presence of the human body still significantly affects propagation mechanisms, primarily through creeping-wave propagation, diffraction, and partial absorption within superficial tissue layers such as skin and subcutaneous tissue.

The total path loss in this scenario can be modeled as a combination of free-space propagation losses and additional attenuation caused by interaction with the human body:

$$L(d) = 20\log_{10}\left(\frac{4\pi d}{\lambda}\right) + L_{\text{body}} + X_{\sigma} \quad (10)$$

where: d represents the distance between the sensors measured along the body surface, L_{body} denotes deterministic body-related losses, and X_{σ} is a log-normal random variable used to model shadowing effects. At WBAN operating frequencies (e.g., 402–405 MHz or 2.4 GHz), two dominant propagation mechanisms are present: the direct LOS component and surface waves (creeping waves) propagating around the curved body surface. These waves enable communication even when geometric visibility is partially obstructed, although they introduce additional attenuation that increases exponentially with angular distance around the body. The value of L_{body} typically ranges from 5 to 20 dB for communication distances spanning several tens of centimeters up to approximately one meter [8]. Due to the relatively short separation distances between sensors (typically 0.1–1 m), free-space propagation losses remain moderate. For example, at a frequency of 403 MHz ($\lambda \approx 0.74$ m), the Friis model yields $L_{FS} \approx 10\text{–}25$ dB for typical WBAN communication distances. Channel variability is commonly modeled using a log-normal distribution, $X_{\sigma} \sim \mathcal{N}(0, \sigma^2)$ where the standard deviation σtypically ranges from 3 to 8 dB, depending on body movements and environmental conditions. The channel is generally considered quasi-stationary, with slow temporal variations caused by user motion.

Scenario V: Body Surface-to-Body Surface NLOS Communication

The communication link between sensors positioned on the body surface under non-line-of-sight (NLOS) conditions represents one of the most challenging scenarios in WBAN systems. In this case, the direct electromagnetic component between the transmitter and receiver is obstructed by parts of the human body, causing signal transmission to rely predominantly on diffraction, reflections, and creeping-wave propagation along the curved body surface. These propagation mechanisms introduce additional losses and greater channel variability compared to the LOS scenario. The total path loss in NLOS on-body communication can be modeled as:

$$\mathrm{L}(d) = 20\log_{10}\left(\frac{4\pi d}{\lambda}\right) + L_{\mathrm{body,NLOS}} + X_\sigma \quad (11)$$

where $L_{\mathrm{body,NLOS}}$represents additional losses caused by body obstruction.

The dominant transmission mechanism in this scenario is creeping-wave propagation, in which electromagnetic waves propagate around the curved surface of the human body. This phenomenon can be approximated by an exponential attenuation model: $E(d) \sim e^{-\beta d}$, where $\beta$is the effective attenuation coefficient dependent on operating frequency, body radius, and the electromagnetic properties of skin and subcutaneous tissues. Since the signal must propagate around the body, the effective propagation path becomes longer, resulting in significantly greater attenuation compared to the LOS scenario. Furthermore, due to complete or partial obstruction of the direct propagation path, diffraction around body edges and reflections from the surrounding environment play an important role, introducing additional signal fluctuations. These effects are commonly modeled through an increased deterministic loss component $L_{\mathrm{body,NLOS}}$, which in practice typically reaches values between approximately 15 and 30 dB depending on body geometry and sensor placement.

Channel variability under NLOS conditions is more pronounced than in LOS scenarios, with the standard deviation commonly reaching values between 6 and 10 dB, reflecting the influence of body motion, posture changes, and multipath propagation effects [10]. Although the channel remains quasi-stationary, it exhibits significantly larger temporal variations.

Scenario VI: Body Surface-to-External Sensor LOS Communication

This scenario represents a propagation case in which the electromagnetic wave transitions from the immediate vicinity of biological tissue into free space and propagates toward an external sensor. Although the direct radio-wave component is dominant in this case, the initial radiation conditions are strongly influenced by the interaction between the antenna and the human body. Consequently, the effective communication channel deviates from the ideal free-space model and includes additional losses and channel variations. In the literature (e.g., IEEE 802.15.6 and measurement-based models at 2.4 GHz), this channel is commonly modeled as a quasi-free-space propagation channel with log-normal shadowing:

$$L(d) = L(d_0) + 10n_{ext}\log_{10}\left(\frac{d}{d_0}\right) + X_\sigma \quad (12)$$

pri čemu je

$$L(d_0) = 20\log_{10}\left(\frac{4\pi d_0}{\lambda}\right) + L_{body} \quad (13)$$

In this model, the key aspect is that L_{body} represents an approximately constant correction factor (for a given antenna position), rather than a distance-dependent function. Therefore, the overall distance dependence remains logarithmic, characterized by a path loss exponent of approximately $n_{\mathrm{ext}} \approx 2$–2.7 [11].

Scenario VII: Body Surface-to-External Sensor NLOS Communication

In this scenario, the communication link is characterized by the absence of a dominant direct propagation component between the transmitter positioned on the body and the external receiver, while the human body acts as the primary obstacle to signal propagation. Under such conditions, the electromagnetic wave reaches the receiver through a combination of diffraction around the body, reflections from the surrounding environment, and, to a lesser extent, transmission through biological tissue. For communication distances within the range of $d = 0.05\,\text{m}$ to $5\,\text{m}$, the channel is still most commonly modeled statistically, although with parameters that significantly differ from the LOS case. The mean path loss is described using a log-normal model:

$$L(d) = L_{ext}(d_0) + 10n_{ext}^{NLOS}\log_{10}\left(\frac{d}{d_0}\right) + X_\sigma \tag{14}$$

where the reference loss $L(d_0)$ incorporates the effects of initial radiation in the vicinity of the human body and the absence of a direct propagation path even at short distances. Unlike the LOS scenario, this term is increased due to additional attenuation caused by body shadowing. The propagation exponent $n_{\text{ext}}^{\text{NLOS}}$ reflects the combined effects of diffraction and multipath propagation, and therefore assumes values greater than those observed in free-space propagation, typically within the range $n_{\text{ext}}^{\text{NLOS}} \approx 3\text{–}4$ [12]. Furthermore, the log-normal random variable $X_\sigma \sim \mathcal{N}(0, \sigma^2)$ exhibits greater dispersion, indicating increased channel variability. From a physical perspective, the total attenuation can be interpreted as the superposition of multiple propagation mechanisms. Diffraction around the human body may be approximated using the Uniform Theory of Diffraction (UTD), where the signal amplitude decreases according to an additional factor dependent on body curvature and the electromagnetic properties of biological tissues. In simplified form, the diffraction contribution may be expressed as an additional loss term:

$$L_{diff} = \propto 20\log_{10}(d) + \Delta_{body} \tag{15}$$

where $\boldsymbol{\Delta}_{\text{body}}$ depends on body geometry and operating frequency. Reflections from walls and surrounding objects introduce multiple propagation paths of different lengths, resulting in interference effects and fluctuations of the received signal. Consequently, the overall channel can be effectively described as a superposition of a large number of weaker propagation components without a dominant direct path.

2. SIMULATION ENVIRONMENT PARAMETERS

The positions of the sensor nodes and their exact coordinates in the 3D space for the WBAN network shown in Figure 1 are presented in Table 1. Within the coordinate system, individual sensor positions with coordinates (x [m], y [m], z [m]) are defined relative to an average human body model (Figure 2). The coordinate system is defined such that the z-axis represents the vertical body axis, i.e., the height of the sensor relative to the ground surface. The coordinate values along the z-axis increase from the feet toward the head. The x-axis represents lateral displacement with respect to the central body axis. Positive values of the x-axis correspond to the right side of the body, whereas negative values correspond to the left side of the body.

The y-axis defines the sensor position relative to the front and back sides of the body. Positive values of the y-axis correspond to sensors positioned on the front side of the body, while negative values represent sensors located on the back side of the body. Such a coordinate system enables precise spatial modeling of sensor placement and facilitates accurate calculation of inter-sensor distances, propagation paths, and path loss values for different WBAN communication scenarios.

In addition, the adopted 3D representation allows realistic simulation of LOS and NLOS propagation conditions, including body-shadowing effects and variations in antenna orientation. The selected sensor positions correspond to typical locations used in medical monitoring systems, such as chest, abdomen, back, arms, and lower extremities, thereby providing a realistic approximation of practical WBAN deployments. Furthermore, the proposed spatial model enables analysis of the influence of body geometry and sensor distribution on the overall communication reliability and energy efficiency of the network.

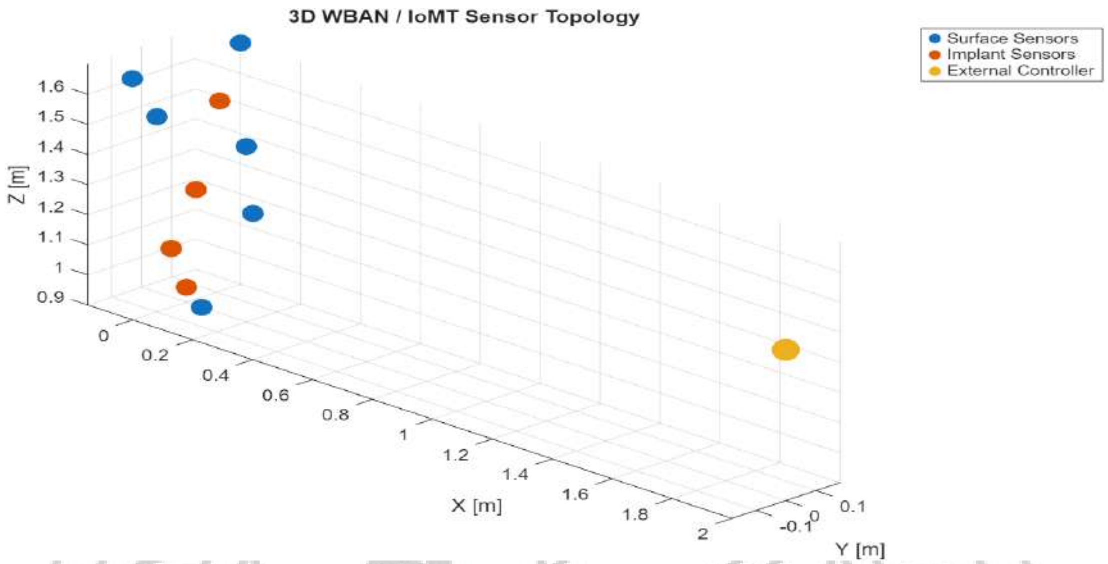

Figure 2. 3D Model of the WBAN Network

The sensor coordinates are defined in meters and are adjusted according to the average anthropometric dimensions of an adult human with an approximate height of 1.75 m. The adopted body model represents a simplified but realistic approximation of the human anatomy commonly used in WBAN propagation studies and simulation environments. Sensor positions were selected in accordance with typical medical and physiological monitoring applications, including cardiac monitoring, body temperature measurement, respiratory monitoring, glucose sensing, and motion tracking.

The spatial distribution of the sensors enables analysis of both short-range and medium-range communication links across different parts of the body. In addition, the selected coordinates allow the investigation of various propagation conditions, including direct line-of-sight communication, body-shadowing effects, and signal propagation around curved body surfaces. The use of a standardized anthropometric model also improves the repeatability and comparability of simulation results with existing WBAN studies presented in the literature.

Table 1:

Node Number	Node Type	Position	x(m)	y(m)	z(m)
1	Implant	chest / heart	0.00	0.02	1.25
2	Implant	chest / lungs	0.08	0.03	1.30
3	Implant	abdomen	0.00	0.02	1.00
4	Implant	hip	-0.08	0.01	0.85
5	Surface	chest – front side	0.00	0.14	1.28
6	Surface	forehead – front side	0.00	0.13	1.68
7	Surface	arm – front side	0.28	0.05	1.10
8	Surface	finger / hand – front side	0.38	0.03	0.95

9	Surface	back – rear side	0.00	-0.14	1.25
10	Surface	leg – front side	0.08	0.07	0.55
11	Surface	shoulder – rear side	-0.22	-0.08	1.45
12	External	in front of the body – chest level	0.60	2.00	1.00
13	External	right side of the body	1.20	0.20	1.10
14	External	behind the body	0.00	-2.00	1.00

In order to analyze signal propagation characteristics, an original simulation model was developed in the MATLAB environment, enabling detailed evaluation of the communication characteristics of the proposed scenarios. After defining the network geometry, the mutual distance between the transmitting and receiving nodes is calculated for each communication scenario. Based on the calculated distance, operating frequency, and communication scenario type, the fundamental signal attenuation is determined using propagation models defined by the IEEE 802.15.6 standard. The simulation model incorporates both deterministic and statistical channel components, allowing realistic representation of propagation effects caused by the human body and surrounding environment.

Within the simulation framework, a comparative analysis of multiple wireless communication technologies commonly employed in IoMT systems was also performed. The analyzed technologies include WiFi, Bluetooth, ZigBee, and MICS, which differ in terms of operating frequency, communication channel bandwidth, data transmission rate, and transmission power. For each technology, the total path loss, received signal power, signal-to-noise ratio (SNR), bit error rate (BER), energy per bit, and specific absorption rate (SAR) were calculated.

The developed MATLAB model enables simultaneous evaluation of communication reliability, energy efficiency, and electromagnetic exposure for different WBAN configurations. In addition, the simulation environment allows investigation of the influence of sensor placement, propagation conditions, and communication technology selection on the overall performance of IoMT systems. Such an approach provides a realistic basis for optimization of WBAN architectures intended for medical monitoring and healthcare applications.

3. SIMULATION RESULTS

For each scenario, system performance was evaluated using different wireless technologies, including WiFi, Bluetooth, ZigBee, and MICS. Figure 3 presents the obtained results for all combinations of communication scenarios and wireless technologies. Specifically, Figure 3 illustrates the total signal attenuation for all sensor nodes within the WBAN/IoMT network when employing the four analyzed wireless technologies: WiFi, Bluetooth, ZigBee, and MICS. The horizontal axis represents the individual sensor nodes, while the vertical axis shows the total signal attenuation expressed in decibels [dB]. The presented results enable direct comparison of propagation losses under different communication conditions and operating frequency bands.

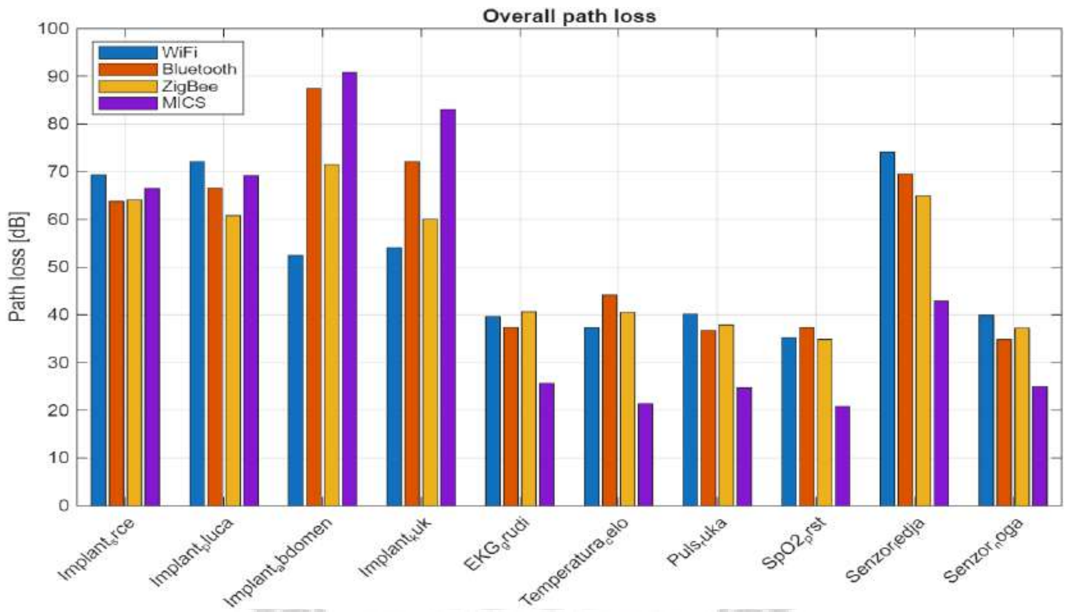

Figure 3. Overall pathloss

The obtained results demonstrate that implantable sensors experience significantly higher attenuation values compared to body-surface sensors. The highest path loss values are observed for the “Implant Abdomen” and “Implant Hip” sensors, particularly when MICS and Bluetooth technologies are employed. This behavior is primarily caused by the fact that signals originating from implantable sensors must propagate through multiple layers of biological tissue, including skin, adipose tissue, and muscle tissue, resulting in substantial absorption of electromagnetic energy. Furthermore, implantation depth additionally increases the overall attenuation. For implantable sensors, it can also be observed that MICS technology, in certain cases, exhibits higher total path loss values than technologies operating at 2.4 GHz. This behavior is a consequence of the specific parameters used in the simulation model, including additional stochastic shadowing components and different propagation model coefficients defined for implant communications. Although lower frequencies generally provide superior propagation characteristics through biological tissues, the overall result also depends on the specific model parameters and additional losses incorporated into the simulation. Body-surface sensors positioned on the front side of the body, such as “ECG Chest,” “Pulse Arm,” and “SpO2 Finger,” exhibit considerably lower attenuation values. These sensors operate under LOS conditions, where an approximately direct propagation path exists between the sensor and the external device without significant body obstruction. Consequently, the total path loss is reduced and the communication link becomes more stable. The most pronounced difference between LOS and NLOS conditions can be observed for the “Back Sensor.” Its path loss values are significantly higher than those of the other body-surface sensors, particularly for WiFi, Bluetooth, and ZigBee technologies. The reason is that this sensor is located on the back side of the body, causing the human body to obstruct the direct propagation path toward the external device. Under such conditions, the signal must propagate around the body via creeping-wave mechanisms and diffraction, resulting in additional attenuation. Figure 4 presents the total signal attenuation as a function of the distance between a body-surface sensor and an external device under LOS (Line-of-Sight) communication conditions. The horizontal axis represents the distance between the sensor and the external device within the range from 0.05 m to 5 m, while the vertical axis indicates the total signal attenuation expressed in decibels [dB]. The graph simultaneously illustrates the four analyzed wireless technologies: WiFi, Bluetooth, ZigBee, and MICS.

The results indicate that signal attenuation gradually increases with increasing distance for all analyzed technologies. This behavior is consistent with the fundamental laws of electromagnetic propagation, according to which the received signal power decreases as the separation distance between the transmitter and receiver increases. In the LOS scenario, the direct propagation component dominates, resulting in relatively low overall losses compared to the NLOS case.

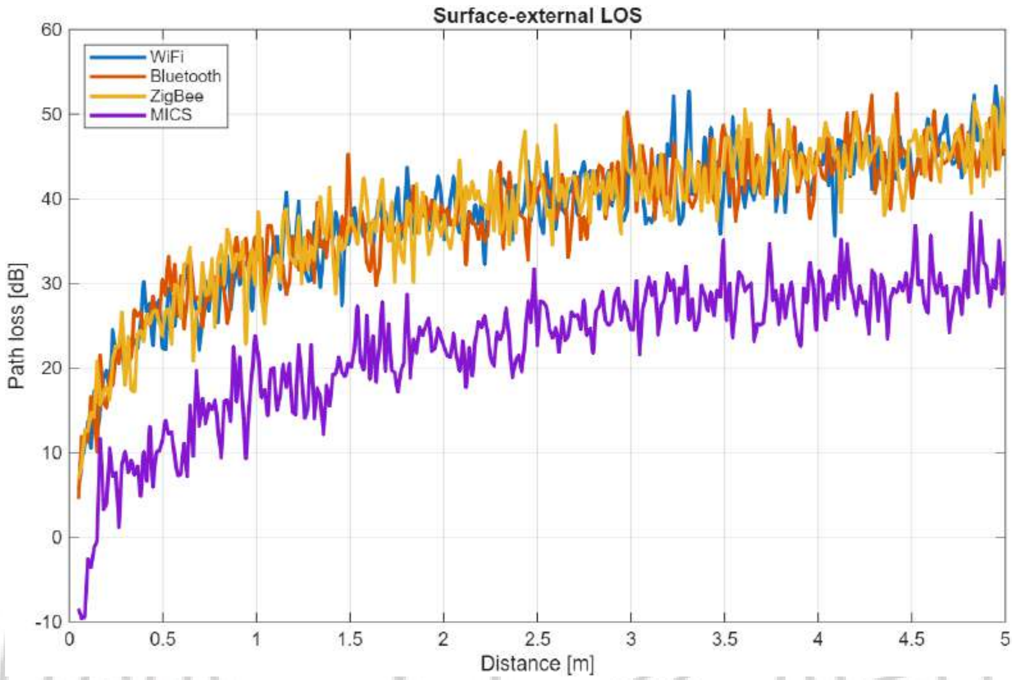

Slika 4. Pathloss in Surface – external LOS scenario

Technologies operating at 2.4 GHz (WiFi, Bluetooth, and ZigBee) exhibit nearly identical attenuation curves, since they utilize the same operating frequency and similar propagation models. The differences between these technologies are not significant within this part of the simulation, because the graph primarily reflects the propagation model rather than transmission power or channel bandwidth characteristics. MICS technology demonstrates lower attenuation compared to the other analyzed technologies. The main reason for this behavior is its lower operating frequency of approximately 403 MHz. Electromagnetic waves at lower frequencies possess more favorable propagation characteristics in the vicinity of the human body and are less susceptible to absorption and diffraction losses. Consequently, MICS achieves more favorable transmission conditions, particularly at larger communication distances.The obtained results confirm that LOS communication between body-surface sensors and external devices represents the most favorable WBAN scenario from the perspective of signal propagation. Under such conditions, stable and energy-efficient communication can be achieved even with relatively low transmission power levels. Path loss values under NLOS conditions are significantly higher than those observed in the LOS scenario. In addition to the fundamental attenuation caused by propagation distance, the simulation model incorporates additional obstruction and shadowing losses representing blockage of the signal propagation path by the human body. As a result, the curves presented in Figure 5 exhibit steeper slopes and higher overall attenuation values.

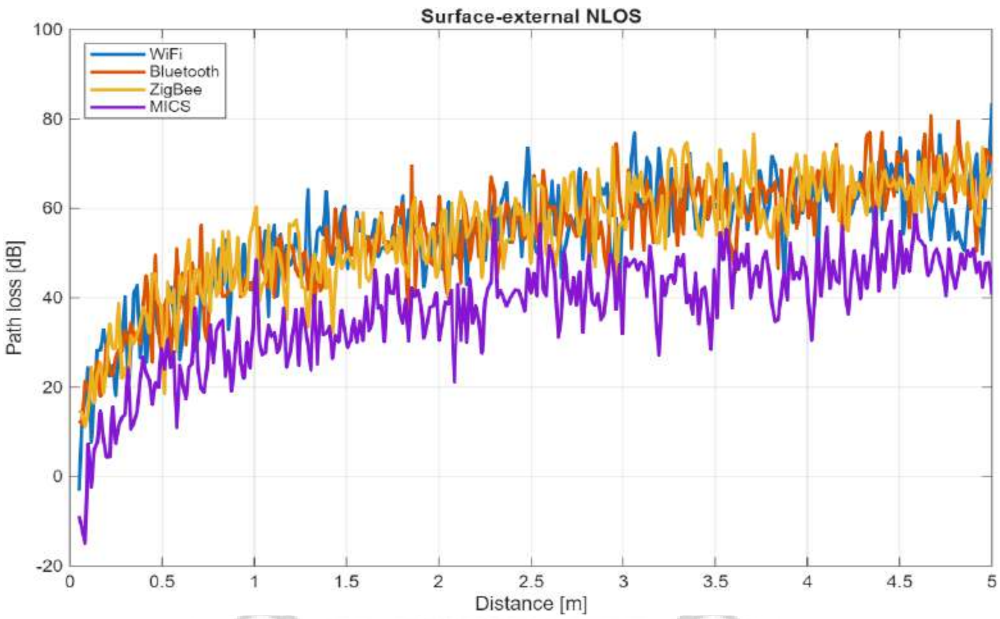

Slika 5. Pathloss in Surface – external NLOS scenario

As in the previous case, WiFi, Bluetooth, and ZigBee exhibit similar characteristics due to their common operating frequency of 2.4 GHz. However, at larger communication distances, their attenuation becomes more pronounced compared to the MICS system. Electromagnetic waves at higher frequencies possess weaker diffraction capability around the human body and experience stronger absorption within biological tissues, making them more sensitive to NLOS propagation conditions. MICS technology also demonstrates the most favorable propagation characteristics in this scenario. Its lower operating frequency enables more efficient propagation around the body and reduced additional losses associated with creeping-wave propagation. These results confirm that lower-frequency communication systems are more suitable for WBAN and implantable medical applications, particularly under complex propagation conditions.

CONCLUSION

In this paper, the characteristics of radio signal attenuation in WBAN/IoMT systems were analyzed for multiple communication scenarios defined by the IEEE 802.15.6 standard. Special attention was devoted to the influence of the human body on electromagnetic wave propagation. Based on an originally developed MATLAB simulation model, a comparative analysis of different wireless technologies, including WiFi, Bluetooth, ZigBee, and MICS, was performed. The simulation results demonstrated that the selection of the operating frequency band, sensor placement, and the presence of obstacles have a significant impact on path loss values, and consequently on communication quality and energy efficiency. The MICS frequency band exhibited favorable characteristics for implantable devices due to its lower operating frequency and reduced attenuation within biological tissues, while ZigBee and Bluetooth proved to be energy-efficient solutions for communication between body-surface sensors. WiFi provides higher data transmission rates, although at the cost of increased energy consumption and higher attenuation in certain communication scenarios. In future research, the authors plan to develop more detailed biomechanical and electromagnetic models of the human body, analyze user mobility and sensor position variations during movement, and investigate the application of machine learning techniques for adaptive optimization of data transmission and energy consumption.

REFERENCES

1. Amiri M, Hamdi A, Meddeb A. Design of wearable antenna sensors and Path loss Modeling for Internet of Wearable Things applications. Research Square; 2023. DOI: 10.21203/rs.3.rs-3110487/v1.
2. J. C. Duncan and N. Ayache, *Medical Image Analysis: Progress Over Two Decades and the Challenges Ahead*, IEEE Transactions on Pattern Analysis and Machine Intelligence, vol. 22, no. 1, pp. 85–106, Jan. 2000.
3. ETSI, “Ultra Low Power Active Medical Implants (ULP-AMI); Part 1: Technical characteristics and test methods,” ETSI EN 301 839-1, V2.1.1, 2019.
4. FCC, *Medical Implant Communications Service (MICS) Rules*, 47 CFR Part 95.
5. Xu, L., Wang, L., et al., “Channel Characterization for In-Body Communication at MICS Band,” *IEEE Transactions on Biomedical Engineering*, 2012.
6. Gabriel, S., Lau, R. W., Gabriel, C. (1996), The dielectric properties of biological tissues: III. Parametric models for the dielectric spectrum of tissues., Physics in Medicine & Biology, 41(11), 2271–2293.
7. Zhang, Y. P., Xiao, S. (2009), On-body and in-body propagation channel modeling for WBAN, IEEE Antennas and Propagation Magazine
8. Alomainy, A., Hao, Y., Hu, X., et al. (2007) Statistical analysis and performance evaluation of on-body radio propagation with microstrip patch antennas, IEEE Transactions on Antennas and Propagation, 55(1), 245–248.
9. S. L. Cotton, W. G. Scanlon, Channel Characterization for Single- and Multiple-Antenna Wearable Systems Used for Indoor Body-to-Body Communications, IEEE Transactions on Antennas and Propagation, 2009.
10. A. Gupta, R. Kumar, and S. Tanwar, “Propagation Characteristics and Path Loss Modeling for WBAN Communications in Healthcare IoT,” *Sensors*, vol. 24, no. 3, Art. no. 1187, 2024.
11. H. Chen, X. Li, and Y. Dong, “Statistical Path Loss Modeling for LOS and NLOS WBAN Scenarios in Healthcare Environments,” *Sensors*, vol. 23, no. 14, Art. no. 6451, 2023.
12. J. Kim, S. Park, and Y. Kim, “Measurement-Based Analysis of Human Body Channel Variability in Dynamic WBAN Environments,” *Electronics*, vol. 13, no. 2, Art. no. 311, 2024.